

Research Article

Design Method of Intelligent Ropeway Type Line Changing Robot Based on Lifting Force Control and Synovial Film Controller

Jiazhen Duan ¹, Ruxin Shi ², Hongtao Liu ¹ and Hailong Rong ³

¹State Grid Changzhou Power Supply Company, Transmission and Distribution Engineering Company, Changzhou, Jiangsu 213000, China

²State Grid Changzhou Power Supply Company, Office, Changzhou, Jiangsu 213000, China

³School of Mechanical Engineering and Rail Transit, Changzhou University, Changzhou, Jiangsu 213164, China

Correspondence should be addressed to Hailong Rong; rhle_16@163.com

Received 25 February 2022; Revised 25 March 2022; Accepted 30 March 2022; Published 12 April 2022

Academic Editor: Shan Zhong

Copyright © 2022 Jiazhen Duan et al. This is an open access article distributed under the Creative Commons Attribution License, which permits unrestricted use, distribution, and reproduction in any medium, provided the original work is properly cited.

Aiming at the problems of low efficiency, reliability, and safety of manual construction for demolition of old lines, a design method of an intelligent ropeway type line changing robot based on lifting force control and synovial film controller is proposed. First, the mechanical model of robot load and line sag is established, and the sag of the overhead line where the robot is located is used to calculate the jacking force that the jacking device needs to provide to the robot. Then, by introducing the radial basis function (RBF) neural network adaptive algorithm into the synovial controller, an adaptive sliding mode position control algorithm based on the RBF neural network is designed to achieve high-precision motion control of the robot in complex operating environments. Finally, based on the compactness, weight, and reliability of the robot, the optimal design is carried out from four aspects of topology, size, shape and morphology, and the design scheme of the robot for wire removal is proposed, and the robot is produced. The developed robot and the other three robots are compared and analyzed under the same conditions through simulation experiments. The results show that the maximum operating time, maximum climbing angle, and maximum traveling speed of the robot developed in this study are all optimal, which are 45 min, 10°, and 1 m/s respectively, and the performance is better than the other three comparison algorithms.

1. Introduction

With the continuous growth of the national electricity demand, more and more transmission lines are put into use. At the same time, there are a large number of old lines. Old lines may affect the safe operation of the power system, personal safety, and property safety [1–3]. At present, the demolition of the old lines of the power grid is basically completed by manual work, and there are many problems such as long construction time, high construction cost, and wide influence range [4, 5]. In view of the above problems, using robots to replace humans to complete construction work such as overhead line demolition and replacement has broad application scenarios and development space and is currently a research hotspot in the industry [6–8].

2. Related Work

Using robots instead of manual construction of the foot frame and completion of the loosening of wire and guide wire back pumping procedures after upping the tower can improve the efficiency of demolition construction and reduce the construction difficulty and cost. It plays a significant role in improving the overall technical level of power line construction [9, 10]. dos Santos [11] developed a rope-climbing robot that can move on distribution lines and the corresponding motion planning to avoid collisions with insulators and other devices. It designs a geometric motion planning control method by using the quintic polynomial interpolation method, so that the robot articulated suspension can retract when approaching obstacles and expand

after crossing obstacles. However, this method does not analyze the accurate control of robot motion speed. In view of the difficulty in calculating the drop of power lines, Zengin et al. [12] proposed a new method to accurately measure the drop of transmission lines based on the power line inspection robot and by using the sensors carried by the robot to collect data and send it remotely. However, this method does not study the motion control method of the robot itself. In view of the problem of poor battery life of the live working robot, Jiang et al. [13] constructed a method to optimize the motion energy consumption of the robot arm. It adapts the genetic algorithm and selects the appropriate algorithm parameters to solve the optimal motion planning of the robot energy consumption, which improves the operation efficiency of the robot. However, this method only takes the lowest energy consumption as the objective function and has limitations. Nguyen et al. [14] developed a robot for cleaning solar panels and simplified it. By establishing the control motion equation of the robot during driving and combining with the linear quadratic regulator, a scheme is proposed to ensure the stable movement of the system and track the desired trajectory. However, this method only focuses on the control method of the robot motion path and cannot guarantee the accuracy of speed control. Aiming at the difficulties and high risks of power grid fault detection, Zhao et al. [15] proposed a patrol robot that can detect equipment faults and identify infrared images of faulty equipment based on infrared imaging technology and support vector machine technology. Although the detection efficiency is enhanced, the accuracy of the method using robots for fault identification is not significantly improved. Xie et al. [16] proposed an integrated 3D printing tube-climbing robot composed of an ordered new soft bending mechanism. The finite element method is used to predict the maximum bending angle of the module, and the output torque and recovery torque are obtained by building a torque test bench. On this basis, the model of the whole robot is established. However, the calculation process of this method is complicated, and the cost is too high to apply in practical engineering. Song et al. [17] proposed an automatic inspection mechanical diagnostic robot based on the fuzzy search method of acoustic signals. The intelligent control of the inspection path of the mechanical diagnostic robot is realized through rough sets, fuzzy neural network (FNN), and self-positioning azimuth correction, and it obtains navigation and search method by using the extracted fault sound signal for fuzzy reasoning. However, this method does not analyze the control complexity and motion accuracy of the robot itself.

Based on the above analysis, in view of the low efficiency and high cost of the current old line dismantling work, a design method of intelligent ropeway type line changing robot based on lifting force control and synovial film controller is proposed. The basic idea is as follows: the mechanical model of robot load and line sag is established to analyze its force and the calculation method of lifting force required by the robot, and by introducing the RBF

neural network into the synovial controller, an adaptive algorithm which can accurately control the robot motion is proposed. Compared with traditional detection methods, the innovations of the proposed method are listed:

- (1) A new method is proposed to calculate the lifting force of the robot. The lifting force required by the robot is calculated based on the vertical radian of the position of the overhead line where the robot is located and the attitude sensor
- (2) The RBF neural network is introduced into the synovial controller, which greatly improves the precision of robot motion control in complex operating environment
- (3) On the basis of not increasing the weight of the robot, the reliability of the robot is improved by optimizing and adjusting the shape, position, and quantity of different structures

3. The Proposed Method

3.1. Automatic Control of Lifting Force Based on Vertical Radian of Overhead Line. When the robot moves on the wire, it needs certain climbing ability to ensure that the wheel will not slide at any time as far as possible, which means that the wheel surface and overhead line are relatively static. This requires that the friction force provided by the driving wheel and the fixed wheel is enough to overcome the influence of the heavy torque and the pulling torque of the rope, so that the robot can remain relatively static [18].

Since the load of the robot is closely related to the sag of overhead line, the mechanical model of the load and sag of the robot should be established first. The statics analysis of the robot is the same in ascending and descending stages. The following is an example of robot climbing. The static model of the robot when it goes uphill is shown in Figure 1.

In Figure 1, M represents the mass of the robot, g represents the acceleration of gravity, v represents the speed of the robot, d_0 represents the distance between the front and rear wheels of the robot, N_f and N_b , respectively, represent the positive pressure of the front and rear wheels of the robot on the line, F_{fs} and F_{bs} , respectively, represent the static friction forces of the front and rear wheels of the robot, M_{s1} and M_{s2} , respectively, represent the braking torque applied by the front and rear wheels of the robot, δ_{fs} and δ_{bs} , respectively, represent the static friction coefficients of the front and rear wheels of the robot, and M_{fs} and M_{bs} are, respectively, the rolling friction moments suffered by the front and rear wheels of the robot, whose values are very small and negligible. It can be regarded as $M_{fs} = M_{bs} = 0$.

Combined with the studies [19, 20] on the dynamic modeling of the shock contact phenomenon in a closed-loop robot chain and the kinetic models based on kinematic control of ellipsoids and cubic nanoparticles, according to Figure 1, the static analysis equation of the robot when it is uphill can be obtained as follows.

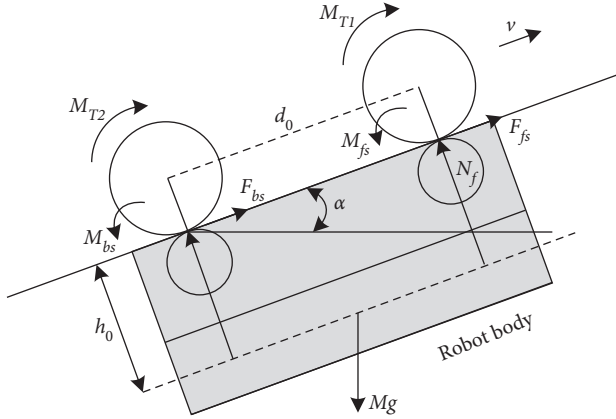


FIGURE 1: Statics model of the robot going uphill.

$$\begin{cases} M_{T1} + M_{T2} - N_f d_0 + Mgh_0 \sin \alpha + \frac{1}{2} Mgd_0 \cos \alpha = 0, \\ F_{fs} + F_{bs} - Mg \sin \alpha = 0, \\ N_f + N_b - Mg \cos \alpha = 0, \\ M_{T1} = F_{fs} r_w, \\ M_{T2} = F_{bs} r_w. \end{cases} \quad (1)$$

In (1), r_w is the angular velocity of the robot wheel.

It can be seen from (1) that in the process of wire climbing, when the driving torque is constant, the running state of the robot is mainly affected by friction. The dip angle of the transmission wire and the support force provided by the lifting device to the driving wheel are two main factors affecting the friction. Therefore, the lifting force required by the lifting device can be calculated by detecting the vertical radian of the position of the overhead wire where the robot is located.

For the robot that adopts the lifting grasping principle with fixed stroke, the friction between the driving wheel and overhead line is constant and cannot be changed according to the change of load, so the adaptability is poor [21, 22]. When the load of the robot is large, because the friction force is not enough to keep the driving wheel and the wire relatively still, it will affect the traveling speed or even cannot climb the slope. In addition, when downhill or under a small load, excessive friction will lead to waste of power and can affect the duration of continuous operation of the robot. Because there are certain differences in the sag of different overhead lines, it is necessary to detect the inclination of the wire before calculating the power required for the robot to move and control the pressure output of the lifting mechanism to adapt to the current load condition.

In order to solve the above problems, the attitude sensor is used to sense the own attitude of robot so as to obtain the inclination of the wire indirectly [23, 24]. The outputs of these sensors are calibrated by the low-power processor in the sensor, and then, these outputs are fused by the

complementary filtering algorithm or extended Kalman algorithm, and the attitude quaternion characterizing the inclination of the transmission wire is obtained. Finally, the attitude quaternion is transformed into Euler angle (pitch angle, roll angle, and azimuth angle) to lay a foundation for the subsequent control of lifting force. The torque to be overcome by the driving wheel is shown in Figure 2.

It can be seen from Figure 2 that the lifting force required to be provided by the two driving wheels is different. After measuring the inclination of the wire, the friction force needed by the driving wheel and the fixed wheel can be calculated combining with the weight of the robot and the real-time drag force of the tow rope, and the lifting force needed by the robot can be calculated on this basis.

The specific design scheme of the lifting force control system is shown in Figure 3. The entire jacking force control system adopts a single closed-loop control method. The control system takes the torque calculation result at the contact point between the driving wheel and the power line as feedback, takes the torque exerted by the driving wheel as the reference, and the difference between the feedback and the reference as the input of the controller, and the output of the controller directly controls the brushless DC. The output of the motor finally achieves the purpose of indirectly adjusting the force of the driving wheel through the electric cylinder. The two driving wheels share a set of torque calculation modules, but the control systems are different. The design of the controller is one of the key points. First, the mathematical model of each part of the brushless DC motor and electric cylinder is constructed, and then, the mathematical model of the controller is constructed by using the automatic control theory, and then, the stability of the controller is analyzed by the Lyapunov method, and other related control theories are used. The robustness and adaptability of the controller are analyzed, and finally, a robust controller is designed.

The entire lifting force control system adopts a single closed-loop control method. The control system takes the torque calculation result at the contact point between the driving wheel and the power line as the feedback and takes the torque exerted by the driving wheel as the input, and the difference between the feedback and the input is the input of the controller. Since the output of the controller can directly control the output of the brushless DC motor, the electric cylinder can indirectly adjust the force applied by the driving wheel.

The two driving wheels share a set of torque calculation modules, and the difference is that their control systems are different. The design process of the controller consists of 4 steps:

- (1) Build the mathematical model of each part of the brushless DC motor and electric cylinder
- (2) Use automatic control theory to build the mathematical model of the controller
- (3) Use the Lyapunov method to analyze the stability of the controller
- (4) Use other related control theories to analyze the robustness and adaptability of the controller

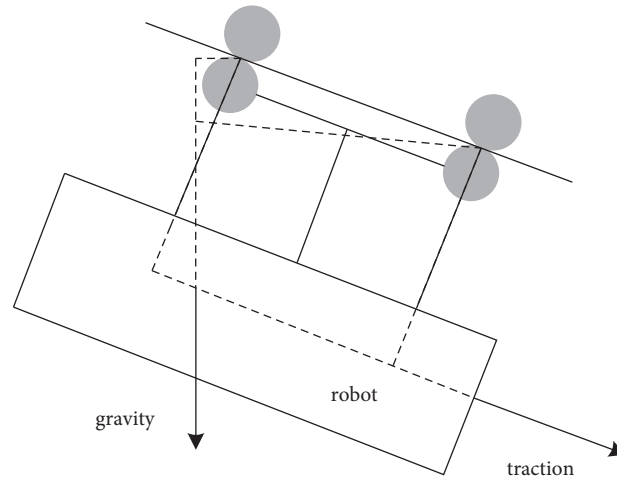


FIGURE 2: The torque to be overcome by the driving wheel.

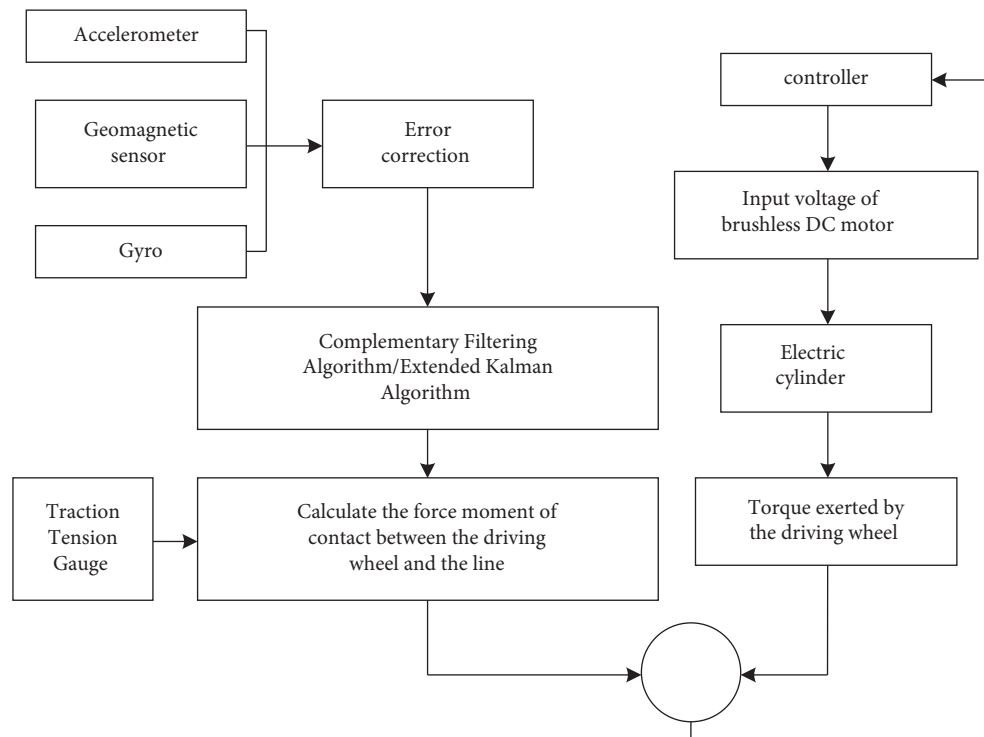


FIGURE 3: The design scheme of the lifting force control system.

3.2. Adaptive Speed Control Based on Neural Network Synovial Controller. When the robot moves along the overhead line, the vertical radius of the overhead line and the length of the traction rope change all the time. In addition, the operating environment is very complicated due to the slippery circuit caused by rain or the swing caused by wind. The complex environment will cause the robot load to change constantly. For the robot controller that realizes speed control through the PID controller, it cannot achieve high-precision speed control in a time-varying environment of load due to its low degree of freedom: when the load of the robot is small, its traveling speed will be fast, which will affect the fastening installation of the hook. When the load of the

robot is large, its traveling speed will be very slow, which will affect the construction efficiency [25, 26]. Therefore, it is necessary to design a more accurate controller to control the walking speed of the robot.

In this study, the speed of the brushless DC motor is controlled by using a synovial controller, so as to achieve accurate control of robot walking speed. The synovial control method for system parameter variations and external disturbances has good robustness and complete adaptability. In practical applications, due to the back-and-forth switching of the control action, the inertia and delay of the system, and the measurement error and other influencing factors, the structure control will appear high-frequency

chattering in the sliding mode, which seriously affects the control performance of the system. It is difficult to solve the above problems only by improving the synovial control method. There will be a static error, and the implementation process of the high-order sliding mode control algorithm is very complicate. So, it is difficult to apply in practice.

This study considers the application of adaptive control idea. Combining the radial basis function (RBF) neural network adaptive algorithm with sliding mode variable structure control, it designs the corresponding RBF neural network adaptive sliding mode position control algorithm and finally realizes the high-precision motion control of the robot in the above complex operation environment. The RBF neural network is an advanced intelligent control algorithm, which has strong self-learning, self-adaptation, and self-organization functions, and has a good application prospect in dealing with nonlinear and uncertain problems of control systems. In addition, the RBF neural network has good approximation ability, simple network structure, and fast learning ability.

The main body of the synovial controller based on the RBF neural network is the synovial controller. By introducing the RBF neural network into the synovial controller, the synovial surface switching function of the controller is adjusted, and the external load disturbance component is added to the switching function. Therefore, the synovial controller generated by modifying the switching function with the neural network becomes an adaptive synovial controller. Once the external disturbance due to the external environment change, the external disturbance will make a sharp change in the switch function of the synovial surface, so that the adaptive synovial controller can respond to the external disturbance quickly and adjust the input current of the brushless DC motor timely; thus, the speed control accuracy is greatly improved.

In order to improve the position control accuracy of the brushless DC motor, the following torque balance equation is given, considering the changes of internal parameters and external loads.

$$\dot{\omega} = -(a + \Delta a)\omega + (b + \Delta b)i - (z + \Delta z). \quad (2)$$

In (2), $a = B/J$, $b = KT/J$, $z = TL/J$. Δa , Δb , and Δz , respectively, represent the disturbance variation caused by the disturbance of the internal parameters of the system and the disturbance of the external load.

In order to make the corresponding angle θ of the position controller track the set angle θ_d faster, the position tracking error of the controller can be expressed as

$$e(t) = x_1 = \theta_d - \theta. \quad (3)$$

At this time, the following equation is established.

$$\begin{cases} e(t) = x_2 = \dot{\theta}_d - \dot{\theta}, \\ \dot{e}(t) = \dot{x}_2 = \ddot{\theta}_d - \ddot{\theta}, \\ = \ddot{\theta}_d + (a + \Delta a)\dot{\theta}_d - (a + \Delta a)x_2 - (b + \Delta b)i + (z + \Delta z). \end{cases} \quad (4)$$

It can be seen from (4) that there is $\dot{e} \rightarrow 0$ when $e \rightarrow 0$, so the position controller meets the design

requirements. At this time, the sliding mode surface switching function is set as

$$s = x_2 + cx_1, \quad c > 0. \quad (5)$$

In (5), $x = [x_1, x_2]^T$ represents the input of the neural network, and c is a constant.

The neural network adaptive sliding mode controller system structure can be divided into three parts: sliding mode variable structure controller, RBF network, and adaptive law.

The input of the neural network will continuously change the size of the weights after learning by the neural network, so that the output function $\hat{f}(x)$ approximates the ideal nonlinear function $f(x)$. The output $\hat{f}(x)$ of the RBF network and the ideal nonlinear function $f(x)$ are shown in the following equations, respectively.

$$\hat{f}(x) = \hat{W}^T h_f(x). \quad (6)$$

$$f(x) = (a + \Delta a)\dot{\theta}_d - (a + \Delta a)x_2 + (z + \Delta z). \quad (7)$$

In (6), $h_f(x)$ is the Gaussian function of the RBF neural network and \hat{W} represents the weighted vector.

In order to further improve the chattering problem of the adaptive sliding mode of the RBF network, the reaching law is optimized, and the optimized reaching law is shown as

$$\dot{s} = -\mu s^2 |s| \text{sgns} - \beta s, \quad \mu > 0, \beta > 0. \quad (8)$$

In (8), the reaching law can be divided into power part and exponential part. When the distance between the moving point of the control system and the sliding mode surface is large, the value of s is large. In this case, the exponential part and the power part work simultaneously and the approaching speed is fast. When $s \rightarrow 0$, the power part tends to zero, and only the exponential part plays a role. The jitter caused by the sign function sgns will diminish with the decrease of the power part. Therefore, the design of approach law not only ensures the convergence speed but also makes the dynamic response of the control system more stable.

Finally, the control law of the system can be obtained as

$$i = \frac{1}{b} [\ddot{\theta} + \hat{f}(x) + cx_2 + \mu s^2 |s| \text{sgns} + \beta s]. \quad (9)$$

Here, the gradient descent method is used to learn the RBF neural network. If the learning rate η is set to a fixed value in the process of weight \hat{W} update, it will cause problems such as low learning efficiency and slow convergence speed. Therefore, the adaptive learning rate is used to adjust the learning rate online, which can speed up the learning rate, while ensuring the stability of the system and the stability of the learning process. The recursive error is

$$E(k) = \frac{1}{2} y(k)^2 - \frac{1}{2} y(k-1)^2. \quad (10)$$

The rules for adjusting the learning rate according to the size of the recursive error are as

$$\begin{cases} \gamma_1 \times \eta(k-1), & (k) < E(k-1), \\ \gamma_2 \times \eta(k-1), & \gamma_3 \times \eta(k-1) < E(k), \\ \eta(k-1), & \text{else.} \end{cases} \quad (11)$$

In (11), γ_1 , γ_2 , and γ_3 are the proportional constants.

Thus, the specific design scheme of the controller can be obtained as shown in Figure 4.

In Figure 4, SMC represents the synovial controller, BLDCM represents the brushless DC motor, the RBF network represents the radial basis function neural network, and adaptive law represents the law of adaptive adjustment.

3.3. Design of Line Changing Robot. The design of the line changing robot needs to ensure the following three technical indicators:

- (1) Compact structure: the uncompact structure of the robot affects the flexibility of its movement and reduces the work efficiency
- (2) Weight size: the weight of the robot will increase the time and energy consumption of the tower up and down, and the high energy consumption during the wiring, and prolong the continuous working time.
- (3) Reliability: improving the reliability of robot operation is very important for safety and maintenance cost reduction in engineering applications
- (4) Mobility: the mobility of a robot affects its adaptability to the operating environment
- (5) Load capacity: in order to ensure the working ability of the robot, the robot also needs to bear the maximum load ≥ 5 kg in addition to carrying its own weight
- (6) Speed requirements: the robot should improve its maximum moving speed as far as possible under the premise of ensuring stability and reliability and reduce the influence of external factors such as wind on work efficiency
- (7) Self-protection ability: in order to prevent the robot from falling, it should have certain safety self-protection measures

Aiming at the above seven indexes, the optimized design is mainly carried out from four aspects of topology optimization, size optimization, shape optimization, and morphology optimization.

Topology optimization: for the critical path of load, aluminum alloy polypropylene composite lightweight laminate is used. For the noncritical path, the polymer plate is used to minimize the bodyweight while ensuring the payload. Designing based on the payload transfer path and optimal material distribution can improve the overall structure and reduce the overall design cost.

Dimension optimization: the volume of robot parts is set as the objective function, and the combination of optimal design parameters is calculated based on dimension

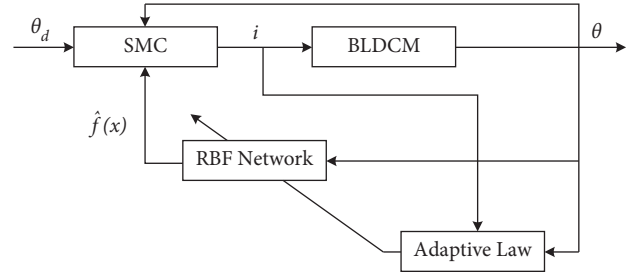


FIGURE 4: Design scheme of synovial controller based on the neural network.

parameters of robot parts such as thickness of plate and section area of pillar.

Shape optimization: based on the designed robot topology, the geometry of different parts is optimized to improve the strength of parts.

Morphology optimization: based on the weight of the designed robot, after fixing the weight, adjust the shape, position, and quantity of different concave-convex structures and optimize the stiffness and mode of sheet metal structural parts, so as to eliminate potential weak links and improve the robot the purpose of reliability.

The main process of robot design includes software and hardware design. The hardware design includes the four aspects:

- (1) Hardware design of robot ontology structure
- (2) Hardware design of the robot control system
- (3) The design of the main control module and the peripheral basic hardware circuit
- (4) Hardware circuit design

The specific design content is given in Table 1.

The hardware design drawing and the line changing robot obtained are shown in Figures 5 and 6, respectively.

The software design mainly includes the realization of the robot control system, the display of robot running state, and the realization of robot remote control. The control flowchart of the line changing robot is shown in Figure 7. The workflow of robot mainly includes the following steps:

- (1) First initialize the robot before work, start the subroutine receiving instructions, and connect it with the ground control device
- (2) The robot starts the synovial controller based on the RBF neural network to realize the adaptive speed control at work
- (3) The robot starts the subroutine that collects and sends its own state and the subroutine that collects and sends video and sends the above data information to the ground receiving device
- (4) The robot receives the instruction from the ground and judges the type of the instruction and executes it until it stops working after receiving the disconnected instruction

TABLE 1: The design content of the line changing robot.

	Content	Purpose
1	Simplify	Reduce structural complexity
2	Redundancy	Redundancy of key structural parameters, functional realization
3	Derating	Reduce the failure rate of components
4	Components outline	Control and manage electronic components and mechanical parts
5	Critical and important	Utilize existing resources to improve the reliability of key and important parts
6	Environmental protection	Choose appropriate materials or solutions to requirements of waterproof, electromagnetic protection, ambient temperature, and humidity.
7	Software reliability	By adopting N-version programming and implementing software engineering and specifications to improve critical reliability
8	Packaging, shipping, storage	Determine packaging protection measures, meet shipping, storage requirements
9	Ergonomics	Make the equipment easy to operate and maintain

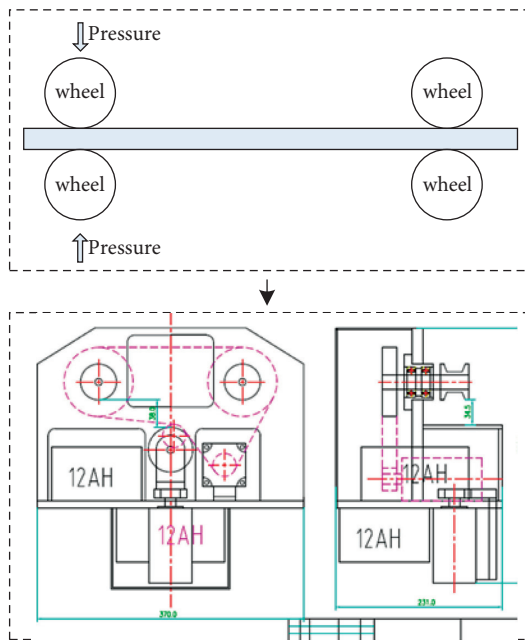


FIGURE 5: Hardware design of line changing robot.

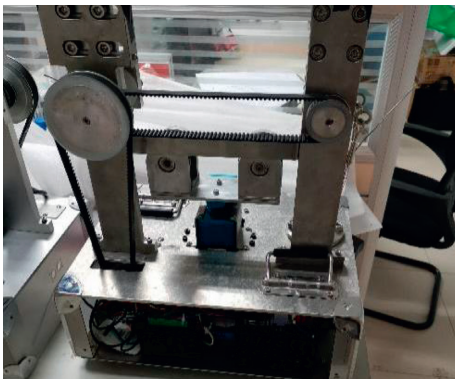


FIGURE 6: Actual object of line changing robot.

4. Experiment and Analysis

4.1. Practical Application Experiment. Some experiments are carried out on the 220 kV overhead transmission line for the designed line changing robot. It is shown in Figure 8.

In the process of practical application, a number of performances of the robot are tested. It measures and analyzes the indicators including the operation success rate of the line changing robot, the online moving speed, the speed control accuracy, the climbing angle, the continuous operation time, and the environmental adaptation.

The experimental results are given in Table 2.

The experimental results show that the robot can move up to 1 m/s, remote control distance up to 1 km, climbing angle up to 10° , continuous operation time up to 45 minutes, and waterproof grade up to 6 on 220 kV and below overhead line. The adaptability of the environment is as follows: it can work normally in the environment, in which the wind is level 5 or less, and the precipitation is 8 ml or less per hour, and the temperature range is $-10\text{--}40^\circ\text{C}$. In addition, the proposed intelligent ropeway type line changing robot based on lifting force control and synovial film controller does not need to build scaffolding and cannot hinder the normal operation of the facilities to be crossed. Compared with on-site construction, the time cost is shortened from days to hours, and the process is fast, efficient, simple, safe, and reliable. It can be reused after a one-time investment, which greatly reduces the cost.

4.2. Performance Comparison Analysis. Since the main external factor affecting the high-altitude operation of robot is the wind, the robot developed in this study and the robot developed in [11, 13, 14] are, respectively, compared and analyzed in terms of operation duration, climbing angle, and traveling speed of the robot under different winds.

The relationship between the maximum operating time, maximum climbing angle, and maximum traveling speed of different robots and wind power is shown in Figures 9–11, respectively.

It can be seen from Figures 9–11 that the developed robot has the largest working time, forward speed, and climbing angle compared with other robots, no matter in no wind or in different wind levels. It indicates that the developed robot is better able to work outdoors at high altitude. The reason is that the sliding mode controller is used to control the robot, and the RBF neural network is introduced in it, which can self-learn, self-adapt, and self-organize to achieve high-precision motion control of the robot in the complex

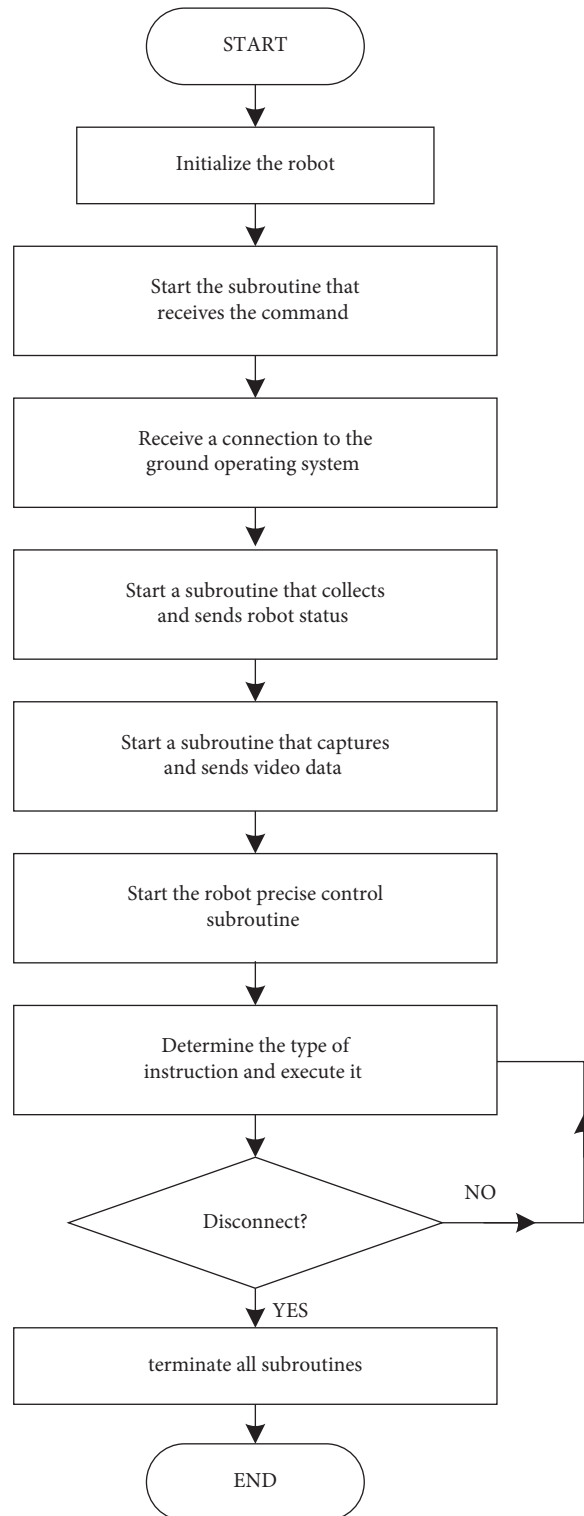


FIGURE 7: Control flowchart of line changing robot.

operation environment. However, the robot developed in [11] does not take into account the accurate control of the robot movement speed. The robot developed in [13] has

good endurance without considering the external environment, but does not consider the performance of other aspects of the robot. The robot developed in [14]



FIGURE 8: Practical application experiment of line changing robot.

TABLE 2: The experimental data of the line changing robot.

Number	Runtime (min)	Success rate (%)	Velocity (m/s)	Climbing angle	Wind	Temperature
1	28	100	0.5	5	2	-3°C
2	30	100	0.6	6	2	-5°C
3	32	100	0.8	5	2	-10°C
4	34	100	1.0	7	3	30°C
5	36	100	0.7	8	4	40°C
6	37	100	0.6	8	5	-7°C
7	40	100	0.8	9	5	-8°C
8	42	100	1.0	10	4	20°C
9	44	100	1.0	10	5	-10°C
10	45	100	1.0	10	3	40°C

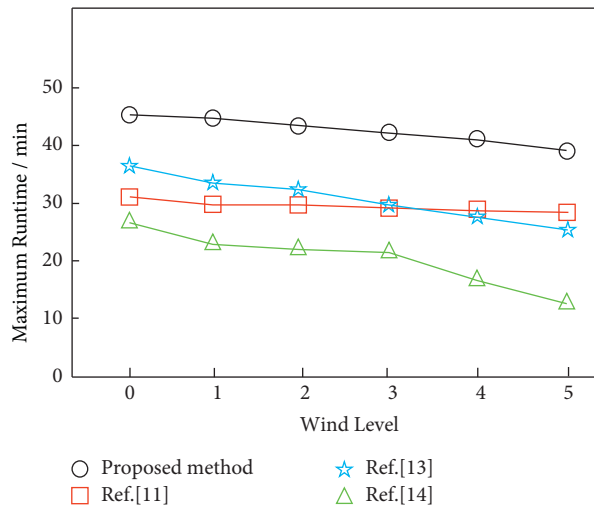


FIGURE 9: The relationship between the maximum runtime of different robots and the wind level.

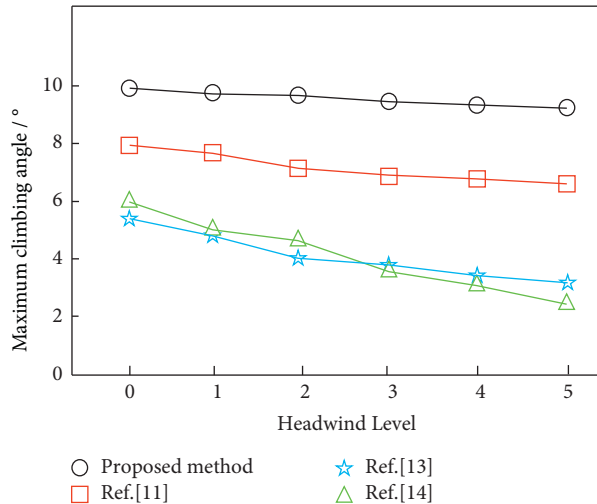


FIGURE 10: The relationship between the maximum climbing angle of different robots and the headwind level.

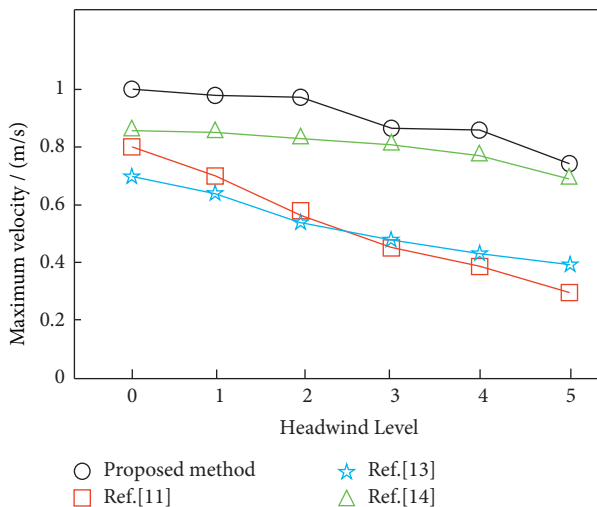


FIGURE 11: The relationship between the maximum velocity of different robots and the headwind level.

overemphasizes the importance of path control while neglects the optimization of the climbing ability of robot speed.

5. Conclusion

To solve the problem of low efficiency in dismantling old lines, an intelligent ropeway line changing robot design method based on lifting force control and synovial controller is proposed. The simulation results are compared between this method and other three methods. The results show that the lifting force required to be provided to the robot can be accurately calculated by using the vertical radian of the overhead line where the robot is located. By introducing the radial basis function (RBF) neural network into the synovial controller, the self-learning and adaptive robot high-precision motion control can be realized. Optimizing the shape, position, and number of different structures without changing the weight of the robot can effectively eliminate

potential weak links and improve the reliability of the robot. In the future, further research will be conducted on the battery module of the line changing robot. Therefore, in the future research on related robots, the RBF neural network can be introduced into the control module to improve the control stability of the robot, and the reliability of the robot can be improved through reasonable structural adjustment and optimization. On the basis of ensuring the good function of the robot, the endurance time of the robot can be extended as far as possible to enhance the ability of its continuous work.

Data Availability

The data used to support the findings of this study are available from the corresponding author upon request.

Conflicts of Interest

The authors declare that they have no conflicts of interest.

Acknowledgments

This work was supported by State Grid Jiangsu Electric Power Co., Ltd. (Incubate project: Research on the Intelligent Cable Method-Based Robot Used for Power Line Removing and Changing under grant JF2021022).

References

- [1] J. Yerramsetti, D. S. Paritala, and R. Jayaraman, "Design and implementation of automatic robot for floating solar panel cleaning system using AI technique," in *Proceedings of the 11th International Conference of Computer Communication and Informatics (ICCCI)*, pp. 105–110, Sri Shakthi Institute of Engineering and Technology, Coimbatore, India, 2021.
- [2] D. Hrubý, D. Marko, M. Olejár, V. Cviklovič, and D. Horňák, "Comparison of control algorithms by simulating power consumption of differential drive mobile robot motion control in vineyard row," *Acta Technologica Agriculturae*, vol. 24, no. 4, pp. 195–201, 2021.
- [3] W. Liao, K. Nagai, and J. Wang, "An evaluation method of electromagnetic interference on bio-sensor used for wearable robot control," *IEEE Transactions on Electromagnetic Compatibility*, vol. 62, no. 1, pp. 36–42, 2020.
- [4] W. Q. Zou, X. Shu, Q. Q. Tang, and S. Lu, "A survey of the application of robots in power system operation and maintenance management," in *Proceedings of the 2019 Chinese Automation Congress (CAC)*, pp. 4614–4619, Hangzhou, China, November 2019.
- [5] M. B. Khan, T. Chuthong, C. D. Do et al., "iCrawl: an inchworm-inspired crawling robot," *IEEE Access*, vol. 8, no. 32, pp. 200655–200668, 2020.
- [6] N. B. David and D. Zarrouk, "Design and analysis of FCSTAR, a hybrid flying and climbing sprawl tuned robot," *IEEE Robotics and Automation Letters*, vol. 6, no. 4, pp. 6188–6195, 2021.
- [7] T. He, Y. Zeng, and Z. Hu, "Research of multi-rotor UAVs detailed autonomous Inspection Technology of Transmission lines based on route planning," *IEEE Access*, vol. 7, no. 3, pp. 114955–114965, 2019.

- [8] Z. P. Wang, B. He, Y. M. Zhou, K. Liu, and C. Zhang, "Design and implementation of a cable inspection robot for cable-stayed bridges," *Robotica*, vol. 39, no. 8, pp. 1417–1433, 2021.
- [9] J. Katrasnik, F. Pernus, and B. Likar, "A survey of mobile robots for distribution power line inspection," *IEEE Transactions on Power Delivery*, vol. 25, no. 1, pp. 485–493, 2010.
- [10] A. Papadimitriou, G. Andrikopoulos, and G. Nikolakopoulos, "On path following evaluation for a tethered climbing robot," in *Proceedings of the 46th Annual Conference of the IEEE-Industrial-Electronics-Society (IECON)*, pp. 656–661, ELECTR Network, Singapore, October 2020.
- [11] C. H. F. dos Santos, M. H. Abdali, D. Martins, and C. B. Aníbal Alexandre, "Geometrical motion planning for cable-climbing robots applied to distribution power lines inspection," *International Journal of Systems Science*, vol. 52, no. 8, pp. 1646–1663, 2021.
- [12] A. T. Zengin, G. Erdemir, T. C. Akinci, and S. Seker, "Measurement of power line sagging using sensor data of a power line inspection robot," *IEEE Access*, vol. 8, no. 5, pp. 99198–99204, 2020.
- [13] W. Jiang, G. C. Ye, D. Zou et al., "Dynamic model based energy consumption optimal motion planning for high-voltage transmission line mobile robot manipulator," *Proceedings of the Institution of Mechanical Engineers, Part K: Journal of Multi-Body Dynamics*, vol. 235, no. 1, pp. 93–105, 2021.
- [14] T. P. Nguyen, H. Nguyen, V. H. Phan, and H. Q. Think Ngo, "Modeling and practical implementation of motion controller for stable movement in a robotic solar panel dust-removal system," *Energy Sources, Part A: Recovery, Utilization, and Environmental Effects*, vol. 23, no. 2, pp. 57–66, 2021.
- [15] X. Zhao, Z. Peng, and S. Zhao, "Substation electric power equipment detection based on patrol robots," *Artificial Life and Robotics*, vol. 25, no. 3, pp. 482–487, 2020.
- [16] D. Xie, J. Liu, R. Kang, and S. Zuo, "Fully 3D-printed modular pipe-climbing robot," *IEEE Robotics and Automation Letters*, vol. 6, no. 2, pp. 462–469, 2020.
- [17] L. Song, H. Wang, and P. Chen, "Automatic patrol and Inspection method for machinery diagnosis robot-sound signal-based fuzzy search approach," *IEEE Sensors Journal*, vol. 20, no. 15, pp. 8276–8286, 2020.
- [18] X. Liu, X. Lu, and S. Zhao, "Kinematics and singularity analysis of an electricity pylon climbing robot," *Journal of Machine Design*, vol. 33, no. 5, pp. 7–13, 2019.
- [19] M. Ahmadizadeh, A. M. Shafei, and M. Fooladi, "Dynamic modeling of closed-chain robotic manipulators in the presence of frictional dynamic forces: a planar case," *Mechanics Based Design of Structures and Machines*, no. 1, pp. 1–21, 2021.
- [20] M. H. Korayem and H. Khaksar, "Estimation of critical force and time required to control the kinematics and friction of rough ellipsoidal and cubic nanoparticles using mechanics of contact surfaces," *Tribology International*, vol. 137, pp. 11–21, 2019.
- [21] X. Lu, S. Zhao, D. Yu, and X. Liu, "Pylon-climber: a novel climbing assistive robot for pylon maintenance," *Industrial Robot: An International Journal*, vol. 44, no. 1, pp. 38–48, 2017.
- [22] A. T. Zengin, G. Erdemir, T. C. Akinci, F. A. Selcuk, M. N. Erduran, and S. S. N. Seker, "ROSETLineBot: one-wheel-drive low-cost power line Inspection robot design and control," *Journal of Electrical Systems*, vol. 15, no. 4, pp. 626–634, 2019.
- [23] T. Q. Mao, K. Huang, X. W. Zeng et al., "Development of power transmission line defects diagnosis system for UAV inspection based on binocular depth imaging technology," in *Proceedings of the 2nd International Conference on Electrical Materials and Power Equipment (ICEMPE)*, pp. 478–481, Guangzhou, China, April 2019.
- [24] M. U. Sumagayan, C. Premachandra, R. B. Mangorsi, C. J. Salaan, H. W. H. Premachandra, and H. Kawanaka, "Detecting power lines using point Instance network for distribution line Inspection," *IEEE Access*, vol. 9, no. 4, pp. 107998–108008, 2021.
- [25] Z. Pu, Y. Xiong, H. Wang et al., "Design and construction of a new insulator detection robot for application in 500 kV strings: electric field analysis and field testing," *Electric Power Systems Research*, vol. 173, no. 7, pp. 48–55, 2019.
- [26] Y. Li, S. He, L. Xu, X. Wang, and A. Zou, "Effect of patrol robot on electric field distribution of human body in 500 kV substation," *Advanced Technology of Electrical Engineering and Energy*, vol. 39, no. 9, pp. 74–80, 2021.